

COMMITTEE

FOR AERONAUTICS

MAILED

JUN 10 1929

JUL 9 1929

TO:

*Library L. M. A. L.*

TECHNICAL NOTES

NATIONAL ADVISORY COMMITTEE FOR AERONAUTICS

No. 310

WIND TUNNEL PRESSURE DISTRIBUTION TESTS ON

A SERIES OF BIPLANE WING MODELS

PART I. EFFECTS OF CHANGES IN STAGGER AND GAP

By Montgomery Knight and Richard W. Noyes  
Langley Memorial Aeronautical Laboratory

**FILE COPY**

To be returned to  
the files of the Langley  
Memorial Aeronautical  
Laboratory

Washington  
July, 1929



NATIONAL ADVISORY COMMITTEE FOR AERONAUTICS.

TECHNICAL NOTE NO. 310.

WIND TUNNEL PRESSURE DISTRIBUTION TESTS ON  
A SERIES OF BIPLANE WING MODELS  
PART I. EFFECTS OF CHANGES IN STAGGER AND GAP.

By Montgomery Knight and Richard W. Noyes.

S u m m a r y

This report furnishes information on the changes in the forces on each wing of a biplane cellule when either the stagger or the gap is varied. The data were obtained from pressure distribution tests made in the Atmospheric Wind Tunnel of the Langley Memorial Aeronautical Laboratory. Since each test was carried up to  $90^\circ$  angle of attack, the results may be used in the study of stalled flight and of spinning as well as in the structural design of biplane wings.

Introduction

This report presents the results of wind tunnel pressure distribution tests which were made in order to determine the magnitude and disposition of the normal or "beam" air loads on two wing models arranged in different biplane combinations. The effects of changes in stagger and gap were investigated separately. A subsequent report, Part II, will cover the results of similar tests in which the decalage, dihedral, sweep-back and overhang were varied.

This investigation forms the second part of a program of force, pressure distribution and autorotation tests on a systematic series of wing models through a large angle of attack range. All the tests are being made in the Five-Foot Atmospheric Wind Tunnel (Reference 1) of the Langley Memorial Aeronautical Laboratory. The force test part of the program has been completed and two reports (References 2 and 3) have been prepared on the results. The autorotation tests are to be made in the near future.

This test program comes under a general study of the aerodynamic factors affecting airplane safety. For this reason, all the tests are carried up to  $90^\circ$  angle of attack.

The information in this report and in Part II may be applied to the structural design of biplane wing systems. The results also have a bearing on safety in stalled flight and on spinning.

### Models and Apparatus

The tests were run on two half-span wing models mounted vertically on a horizontal "separation plane," the assumption being made that the imaginary plane of symmetry of a wing can be replaced by an actual plane surface without changing the flow. The separation plane, if sufficiently large, thus makes it possible to remove half of the wing and to substitute for it the pressure leads and supports for the remaining half. This method of test is frequently used in pressure distribution work.

In order to overcome the frictional reduction in air speed near the separation plane the leading edge of the plane, which consisted of a hinged flap  $5\frac{1}{2}$  inches wide, was bent downward until vertical Pitot-static surveys made about 1 foot upstream from the models showed that the dynamic pressure distribution was satisfactory. A Pitot-static tube installed permanently in the tunnel was calibrated against the final survey. This service instrument was sufficiently far upstream from the models to be unaffected by them, and was used as the dynamic pressure reference in all the tests.

The test models were two 5-inch chord half-span airfoils of aspect ratio 6. Each had circular tips and the Clark Y profile throughout. They were built up of mahogany laminated along the span and the ordinates were within  $+.004$  inch ( $.0008$  chord) of those specified in Table I, except on the lower surface slightly back of the leading edge where a maximum deviation of  $-.010$  inch ( $.002$  chord) was found. After the completion of all the tests the lower wing was found to have developed a negative twist (washout) amounting to fifty minutes of angle at the tip. This twist does not materially affect the results at large angles of attack.

In constructing the airfoils brass tubes of  $.015$  inch inside diameter were inlaid between the laminations. These tubes were brought out flush with the airfoil surface, thus forming the pressure orifices. The orifices were arranged on each wing

in five sections normal to the span. Figure 1 shows the two wing models with base blocks and pressure connections. Figure 2 is the plan view of each wing showing the location of the orifices.

Figure 3 shows the models mounted in the tunnel on the separation plane. The sealing disk turned with the airfoils when the angle of attack was changed. Figure 4 is a general view of the test set-up including the models, separation plane, model bracket, bracket fairing, angle of attack handles, rubber tubes from wing to manometer, and the liquid multiple manometer. The openings shown in the fairing and in the tunnel wall were closed when testing.

The multiple manometer held 130 tubes. Of these 120 were connected to the wing orifices and 10 (2 for each manometer section) were connected to a static orifice in the tunnel wall upstream from the models. The orifice and static pressures were recorded photographically as heads of alcohol by exposing photostat paper stretched over the glass tubes between the two reels mounted in boxes at each end of the manometer. Illumination for the exposure was obtained from a 40-watt lamp located 7 feet to the rear and in the horizontal center plane of the tube-bank.

In order to save time and to increase accuracy in working up the test data, the manometer tubes were located as nearly as possible in the same relative position with respect to each

other as were the orifices along the chord of the wing models. Near the leading edge where the orifices were closely spaced, it was necessary to depart slightly from this arrangement, but the required offsets were taken into account in fairing the records. This method of tube spacing permitted the fairing of the pressure diagrams directly on the photostat records. A reduced copy of a record, cut in half for convenience, with the diagrams faired through the meniscuses is shown in Figure 5. The static pressure lines are shown in white.

### T e s t s

The biplane arrangements tested were divided into two groups as follows:

1. Variation in stagger (gap/chord) = 1,    decalage = 0,  
dihedral = 0,    sweepback = 0,    overhang = 0.)

See Figure 6.

- (a) -25 per cent chord
- (b)    0
- (c) +25 per cent chord
- (d) 50 per cent chord
- (e) 75 per cent chord

2. Variation in gap (stagger = 0,    decalage = 0,  
dihedral = 0,    sweepback = 0,    overhang = 0.)

See Figure 15.

- (a) 50 per cent chord
- (b) 75 per cent chord
- (c) 100 per cent chord
- (d) 125 per cent chord
- (e) 150 per cent chord

Each test was made at angles of attack of  $-8^{\circ}$ ,  $-4^{\circ}$ ,  $0$ ,  $+4^{\circ}$ ,  $8^{\circ}$ ,  $12^{\circ}$ ,  $14^{\circ}$ ,  $16^{\circ}$ ,  $18^{\circ}$ ,  $20^{\circ}$ ,  $22^{\circ}$ ,  $25^{\circ}$ ,  $30^{\circ}$ ,  $35^{\circ}$ ,  $40^{\circ}$ ,  $50^{\circ}$ ,  $60^{\circ}$ ,  $70^{\circ}$ ,  $80^{\circ}$  and  $90^{\circ}$ . The dynamic pressure  $q$ , as measured by the service Pitot-static tube, was maintained at 4.09 lb. per sq.ft., corresponding to an average velocity of very nearly 40 M.P.H., and to a Reynolds Number of about 150,000.

In preparing for each test, the wing models were first clamped in the desired relative position and the space between them was filled with plasticine faired flush with the upper surface of the disk. Each of the 120 pressure lines from orifice to manometer was checked for leaks and possible blocking. The test room was then darkened except for a red light, and the photostat paper was drawn across the manometer tubes. Due to the damping effect of the small bore brass tubes used in the wing, two minutes were allowed for reaching steady conditions for each angle of attack. The time required for the exposure was about one-half second. Following the exposure the angle of attack was changed, a new length of photostat paper reeled in place and the next record was taken.

## R e s u l t s

The results are presented in the form of comparison curves and are divided into two groups. In the first group is shown the way in which the loadings on the wings are affected by changing the stagger, and in the second, by changing the gap. From these curves may be determined the magnitude and point of action of the semi-span normal force on each wing for any reasonable amount of stagger or gap and for most of the angles of attack apt to be encountered in flight. Following is a list of the comparison curves, all of which are plotted against angle of attack: (The first and second figure numbers refer to stagger and gap, respectively).

Figures 7 and 16. Normal force coefficient for cellule.

Figures 8 and 17. Normal force coefficient for upper wing.

Figures 9 and 18. Normal force coefficient for lower wing.

Figures 10 and 19. Ratio of load on each wing to load on cellule.

Figures 11 and 20. Longitudinal center of pressure for upper wing.

Figures 12 and 21. Longitudinal center of pressure for lower wing.

Figures 13 and 22. Lateral center of pressure for upper wing.

Figures 14 and 23. Lateral center of pressure for lower wing.



In order to show the nature of the interference effects on the two biplane wings, each figure, with the obvious exception of Figures 10 and 19, has superimposed upon it the corresponding curve for the monoplane condition. Owing to the slight difference in the two wings, the monoplane curve in Figures 7 and 16 is the average of the monoplane curves for each wing.

The procedure in working up the test data consisted first of drawing the pressure diagrams on the photostat records. These diagrams were then integrated for area and also for moment about the leading edge or, in the case of the two tip sections on each wing, about the main leading edge produced. These integrations were then corrected for photostat shrinkage and plotted versus semi-span. The semi-span load and moment diagrams thus produced were integrated for area and also in the case of the load diagrams for moment about the wing root. The normal force coefficient ( $C_{NF}$ ) for each wing was then calculated from

$$C_{NF} = \frac{2 A_{SL}}{S q}$$

Where, in consistent units

$A_{SL}$  = area of semi-span load diagram

$S$  = area of wing

$q$  = dynamic pressure expressed as a head of the manometer fluid.

The normal force coefficient for the biplane combination was calculated from

$$C_{NF} (\text{cellule}) = \frac{C_{NF} (\text{upper}) + C_{NF} (\text{lower})}{2}$$

The wing load ratios showing the division of the total load between the two wings were determined from:

$$R_u = \frac{C_{NF} \text{ (upper)}}{2 C_{NF} \text{ (cellule)}}$$

$$R_L = \frac{C_{NF} \text{ (lower)}}{2 C_{NF} \text{ (cellule)}}$$

where  $R_u$  = upper wing load ratio  
 $R_L$  = lower wing load ratio.

The longitudinal center of pressure  $C_{px}$ , was obtained from

$$C_{px} = \frac{A_{SM}}{A_{SL} \times C}$$

where  $A_{SM}$  = area of semi-span moment diagram  
 $C$  = basic chord of wing (5 in.).

The equation for the lateral center of pressure  $C_{py}$ , is

$$C_{py} = \frac{2 M_{SL}}{A_{SL} \times b}$$

where  $M_{SL}$  = moment of semi-span load diagram about wing root.  
 $b$  = span of wing.

The average deviation of the curve points on the figures from a mean value was within  $\pm 2$  per cent. This was determined from check tests, fairings, and integrations.

A source of error in tests in a closed throat tunnel at large angles of attack is the constriction of the effective tun-

nel area by the wing model. The constriction increases the effective dynamic pressure at the model. This error and a method of correction for full span wings are described in Reference 3. It appears that the values of  $C_{NF}$  at  $90^\circ$  from the present tests closely check those for the uncorrected force tests in the above reference, and hence a  $C_{NF}$  reduction of about 4 per cent at this angle would appear to be in order. However, the tunnel conditions for the pressure distribution tests are considerably different from those for the force tests, and the blocking correction could be obtained with certainty only by making special blocking effect tests on the pressure distribution set-up. These tests have not been made thus far and so the results in this report are uncorrected for tunnel wall effects. However, the use of the curves for comparison with one another is not affected by this fact.

### D i s c u s s i o n

That the upper wing of a biplane modifies the aerodynamic characteristics of the lower and vice versa is well known. The nature of the flow modification below the angle of maximum lift has been frequently demonstrated by theory and experiment hitherto, and for this reason, only the region from the angle of maximum lift to  $90^\circ$  will be discussed briefly herein.

A monoplane wing at angles of attack above maximum lift produces behind it a turbulent wake having a depth approximately

equal to the projection of the wing normal to the flight path. Also, just in front of the wing the smooth air is deflected downward by the lower surface. With these facts in mind, it is easy to see that the addition of a second wing to the first to form a biplane wing system will modify the flow and hence the forces on the first wing. If the added wing is placed below, the lower surface of the first wing (now the upper wing of the biplane combination) will be working to some extent in turbulent air and the forces on it will, in general, be reduced. It is apparent that the greater the positive stagger or the greater the gap, the less will be this shielding effect. The results shown in Figures 8, 10, 17 and 19 verify these statements.

On the other hand, if the added wing is placed above the first wing, the turbulent region behind the latter (now the lower wing) will be deflected downward and reduced in depth, thus increasing the forces upon this wing. For this arrangement the action of the upper wing on the lower is somewhat analogous to that of the auxiliary airfoil of the Handley Page slot upon the wing behind it. The greater the positive stagger and the less the gap, the greater will be this effect. Figures 9, 10, 18 and 19 will be found to bear out these statements.

A point of interest is the fact that the lower wing characteristics are, in general, much less affected by the interference of the upper wing than vice versa. Also, in general, at large angles of attack increasing the stagger in the positive

sense or increasing the gap tends to equalize the loads on the two wings and also increases the normal force coefficient of the combination.

The data in this report will not at present be discussed from the standpoints of stalled flight and spinning. Such a discussion can better be made later when the autorotation tests mentioned above have been completed.

In interpreting the results of this wind tunnel investigation, the low Reynolds Number of the tests (150,000) should be kept in mind. However, while scale effect will doubtless change the absolute value of the coefficients, the relative changes produced by stagger and gap variations will probably hold for Reynolds Numbers greater than that of the tests.

### C o n c l u s i o n s

The following general conclusions may be drawn relative to the effects of changes in stagger and gap of biplane wings at angles of attack above that of maximum lift.

1. The lower wing characteristics are much less affected by the interference of the upper wing than vice versa.

2. Increasing the stagger in the positive direction or increasing the gap tends to equalize the loads on the two wings and also increases the normal force coefficient of the cellule.

Langley Memorial Aeronautical Laboratory,  
National Advisory Committee for Aeronautics,  
Langley Field, Va., May 22, 1929.

## R e f e r e n c e s

1. Reid, Elliott G. : Standardization Tests of N.A.C.A. No. 1 Wind Tunnel. N.A.C.A. Technical Report No. 195 (1924).
2. Wenzinger, Carl J. and Harris, Thomas A. : Wind Tunnel Force Tests on Wing Systems through Large Angles of Attack. N.A.C.A. Technical Note No. 294 (1928).
3. Knight, Monttgomery and Wenzinger, Carl J. : Wind Tunnel Tests on a Series of Wing Models through a Large Angle of Attack Range, Part I: Force Tests. N.A.C.A. Technical Report No. 317 (1928).

TABLE I.

## Clark Y Airfoil Ordinates

<u>Distance from L.E.</u>	<u>Lower-surface ordinates</u>	<u>Upper surface ordinates</u>
Chord	Chord	Chord
$\left( \frac{\text{LE radius}}{\text{Chord}} = .0150 \right)$		
0	.0350	.0350
.0125	.0193	.0545
.0250	.0147	.0650
.050	.0093	.0790
.075	.0063	.0885
.100	.0042	.0960
.150	.0015	.1069
.200	.0003	.1136
.300	0	.1170
.400	0	.1140
.500	0	.1052
.600	0	.0915
.700	0	.0735
.800	0	.0522
.900	0	.0280
.950	0	.0149
1.000	0	.0012

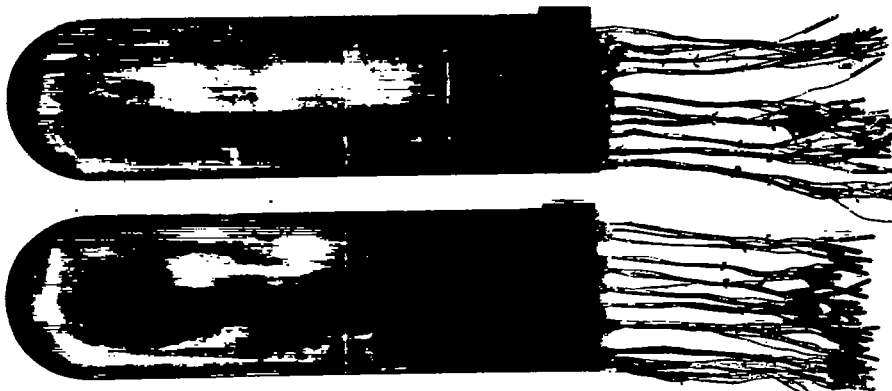


Fig. 1 Half-span pressure distribution wing models.

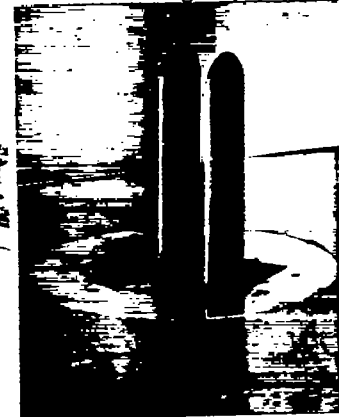


Fig. 3 Biplane wings and separation plane in wind tunnel.

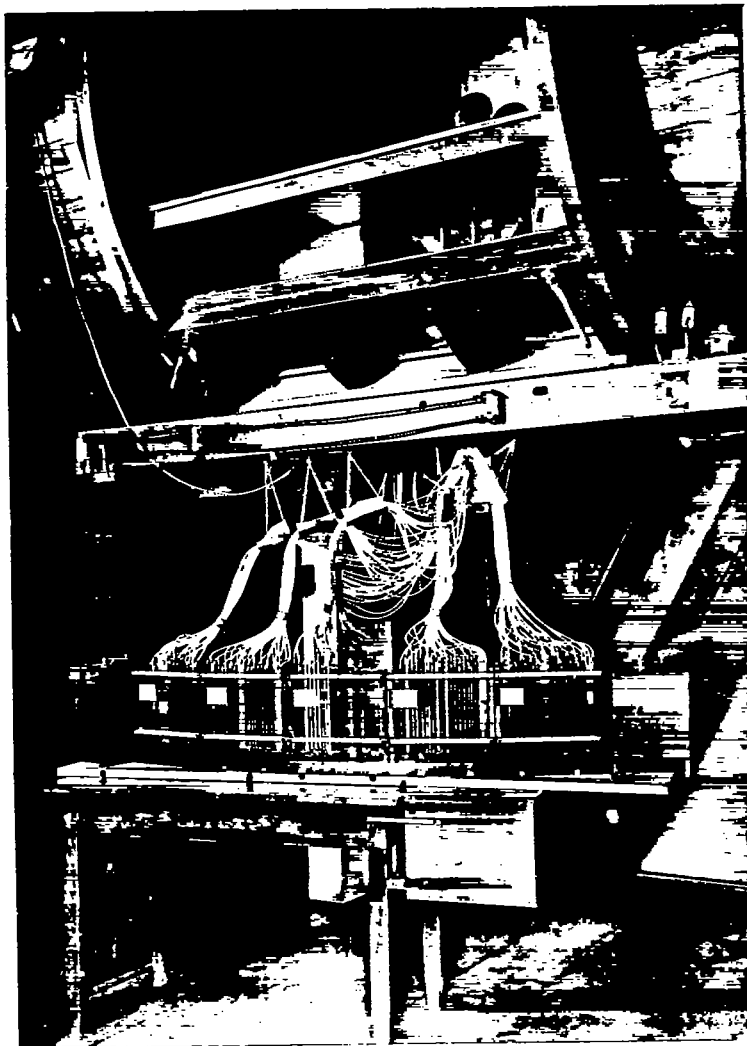


Fig. 4 Biplane pressure distribution apparatus installation in wind tunnel.

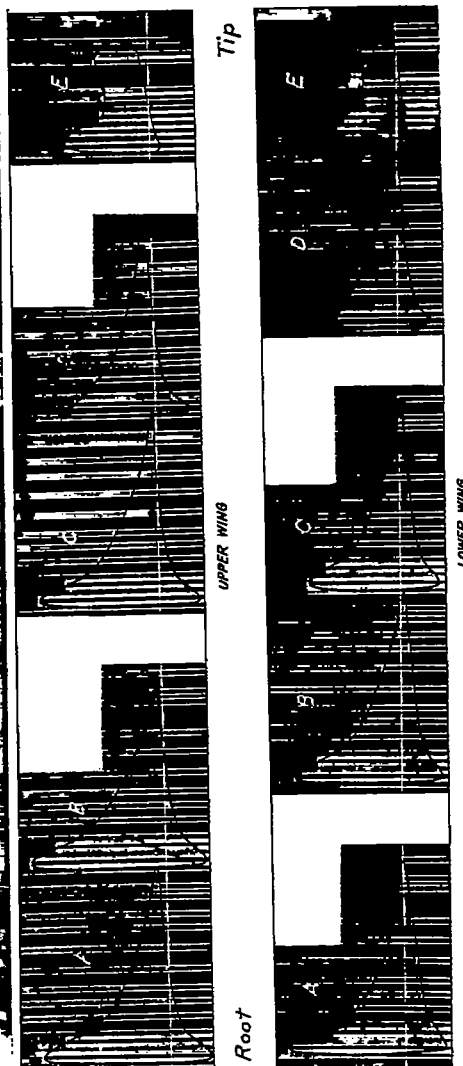


Fig. 5 Biplane photostat manometer record (reduced).  $\alpha = 16^\circ$

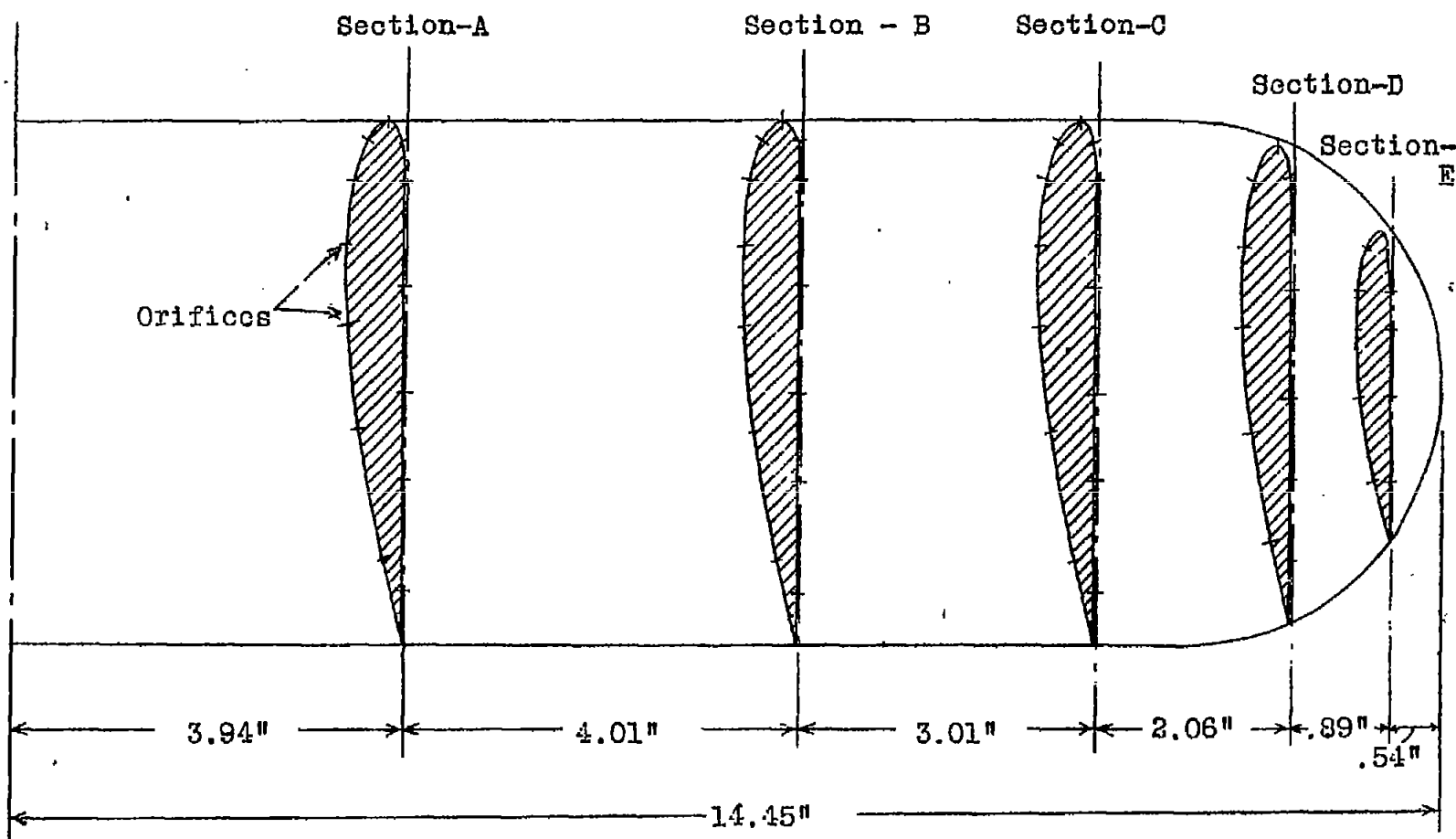


Fig.2 Wing showing orifice locations.



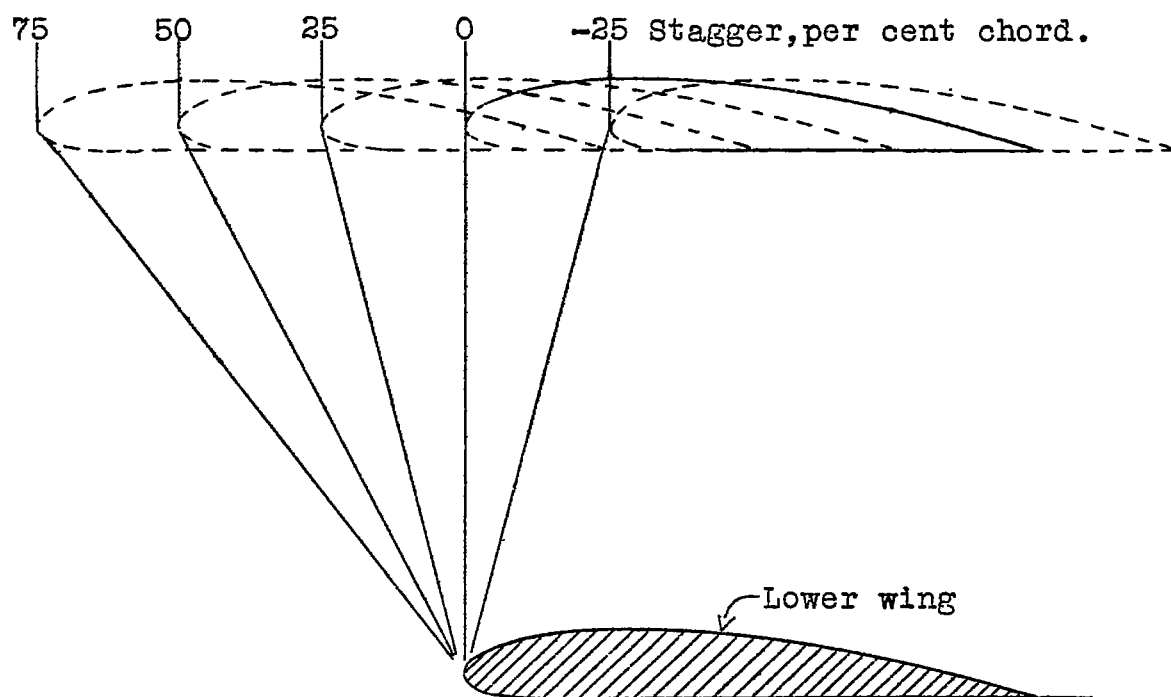


Fig.6 Wing model arrangements used in tests on the effect of variations in stagger.

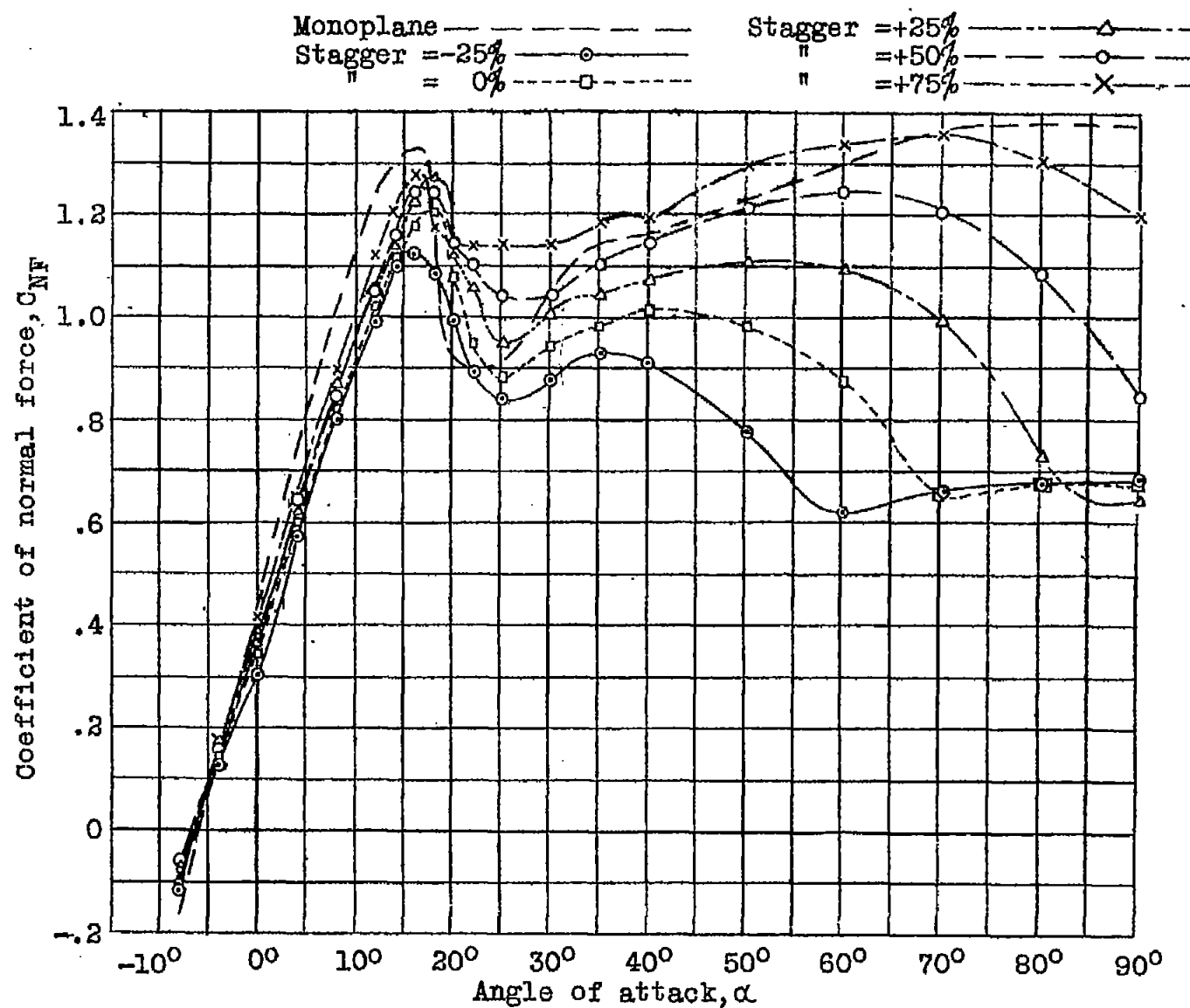


Fig. 7 Effect of stagger on cellule normal force coefficient.

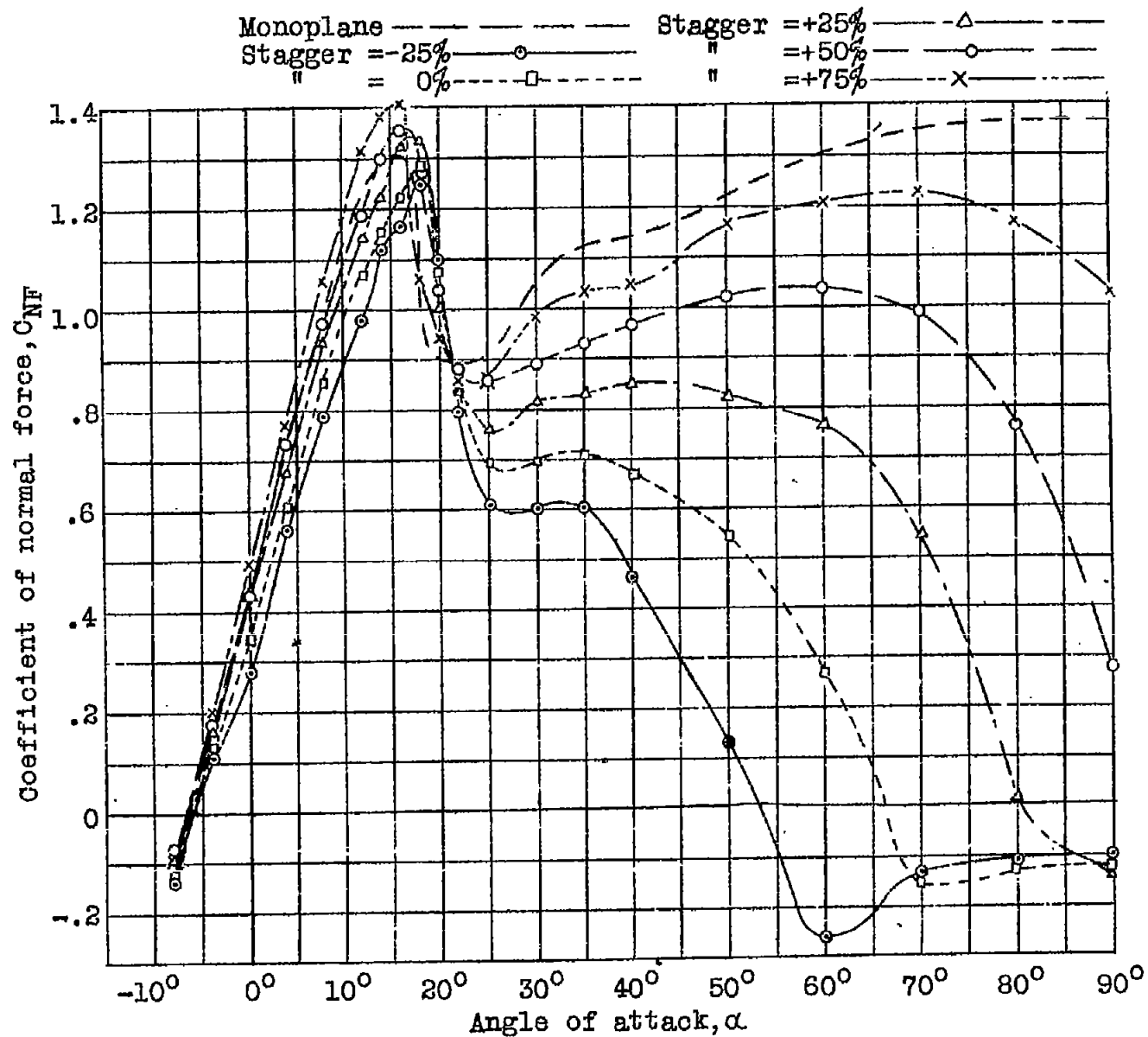


Fig. 8 Effect of stagger on upper wing normal force coefficient.

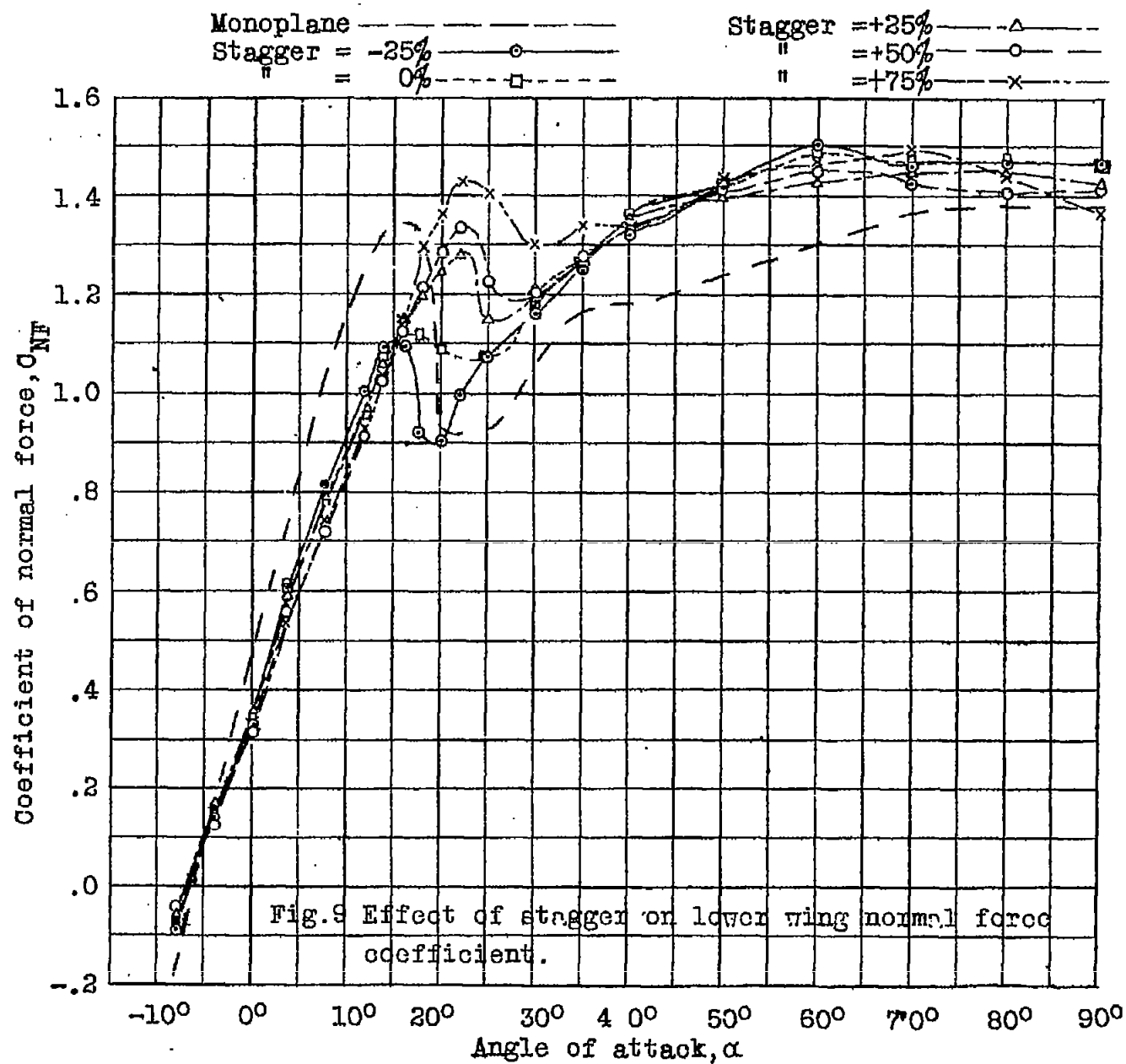


Fig. 9

FIG. 10

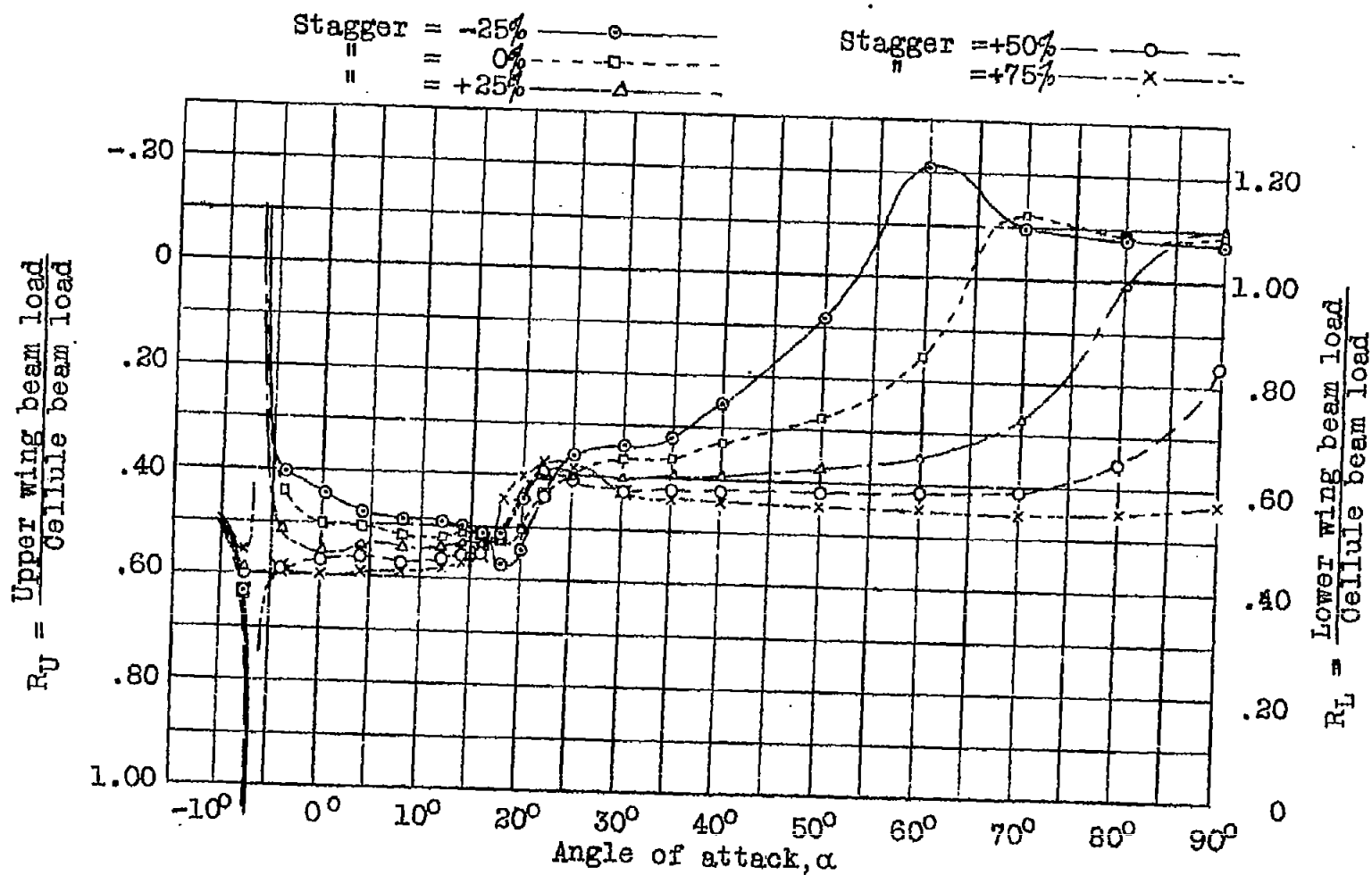
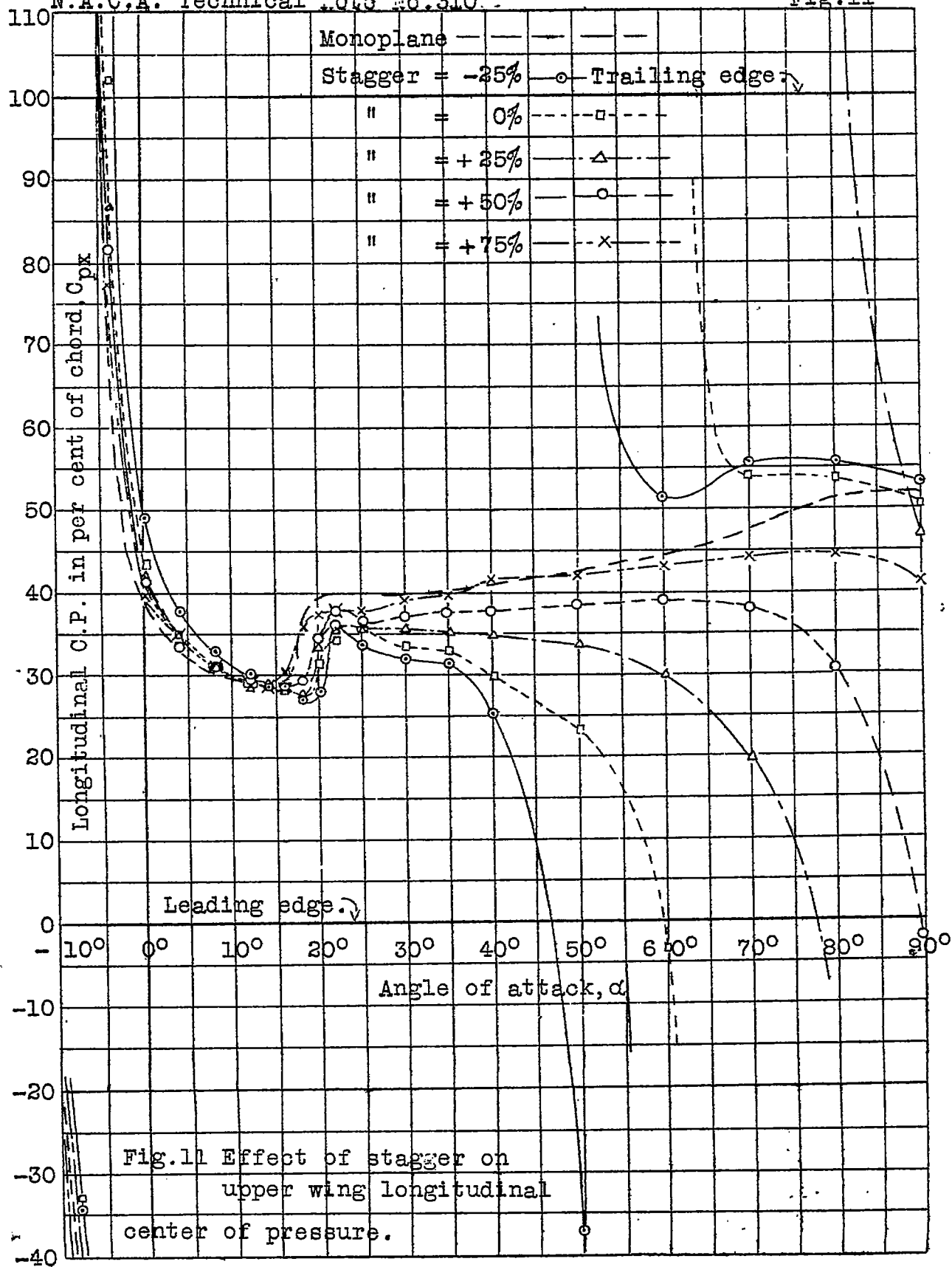
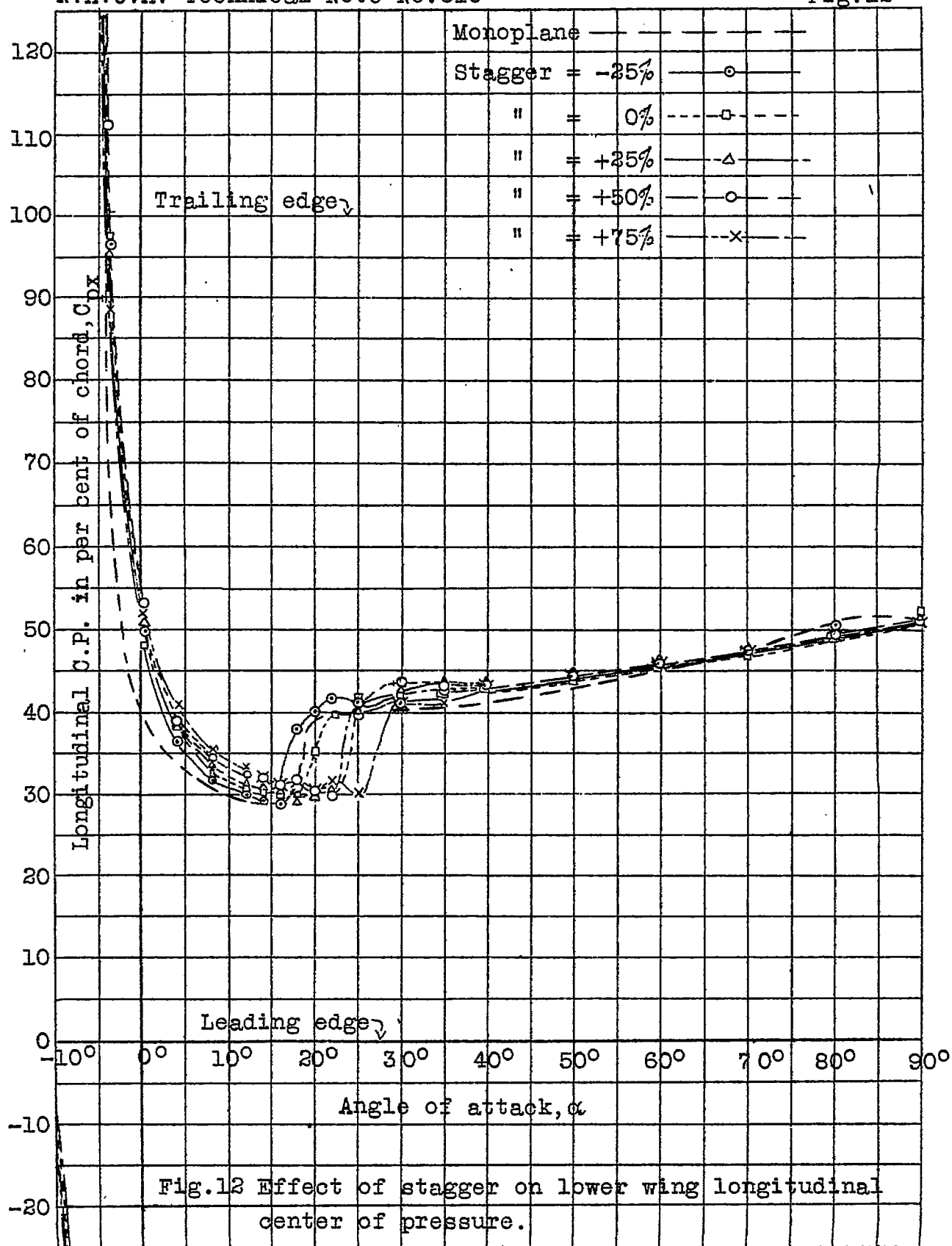
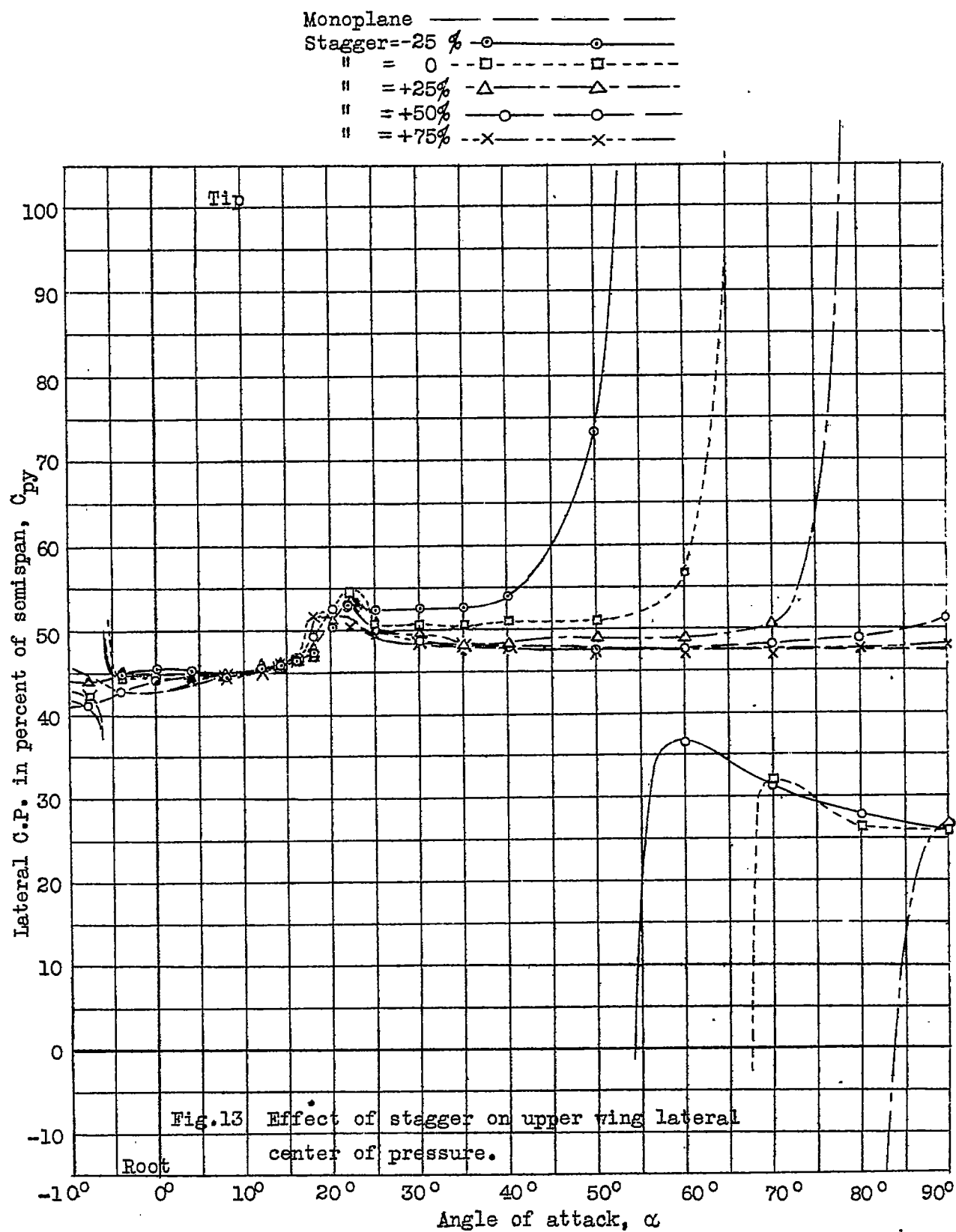


Fig. 10 Effect of stagger on wing load ratio.









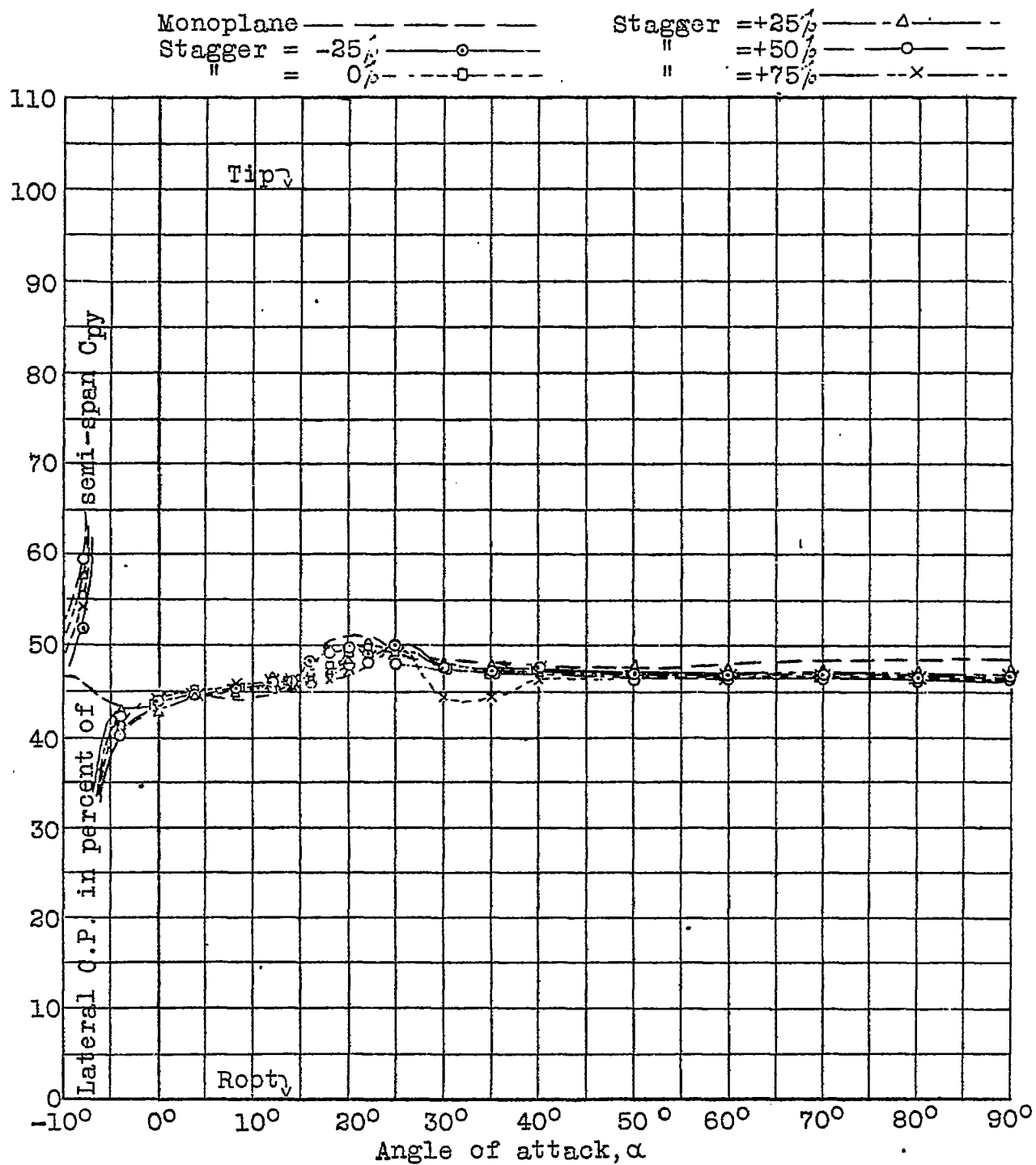


Fig.14 Effect of stagger on lower wing lateral center of pressure.

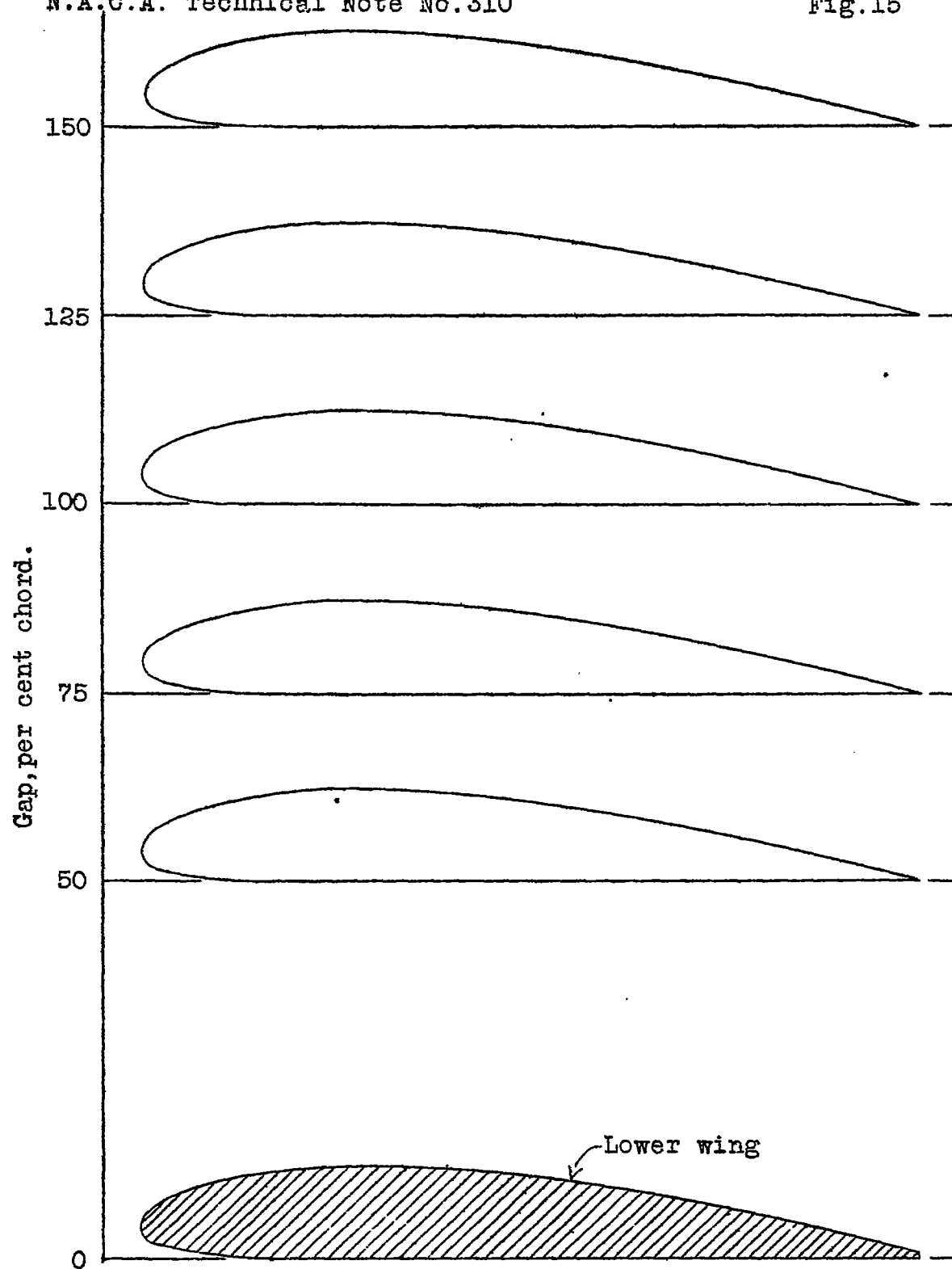


Fig.15 Wing model arrangements used in tests on the effect of variations in gap.

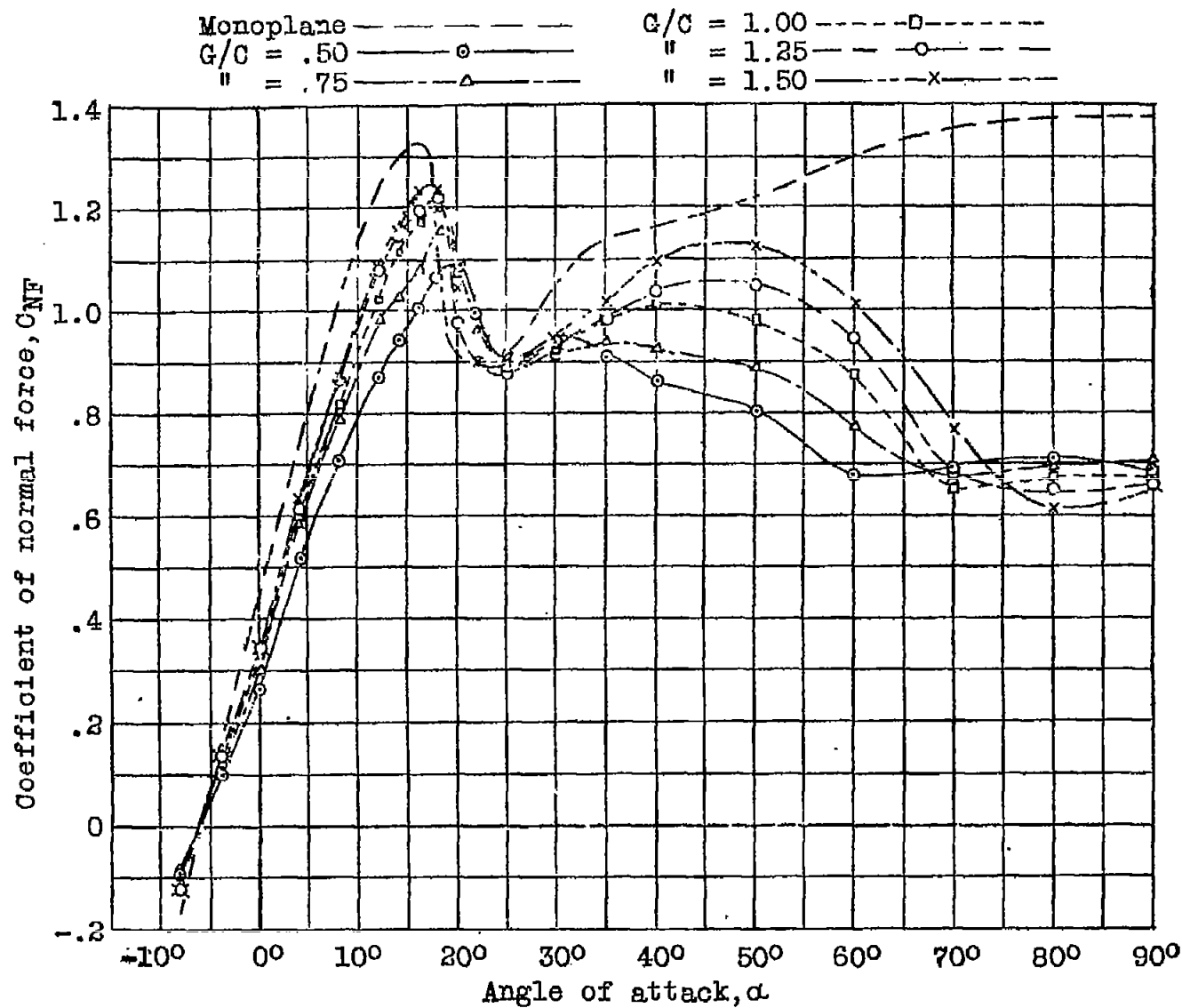


Fig. 16 Effect of gap on cellule normal force coefficient.

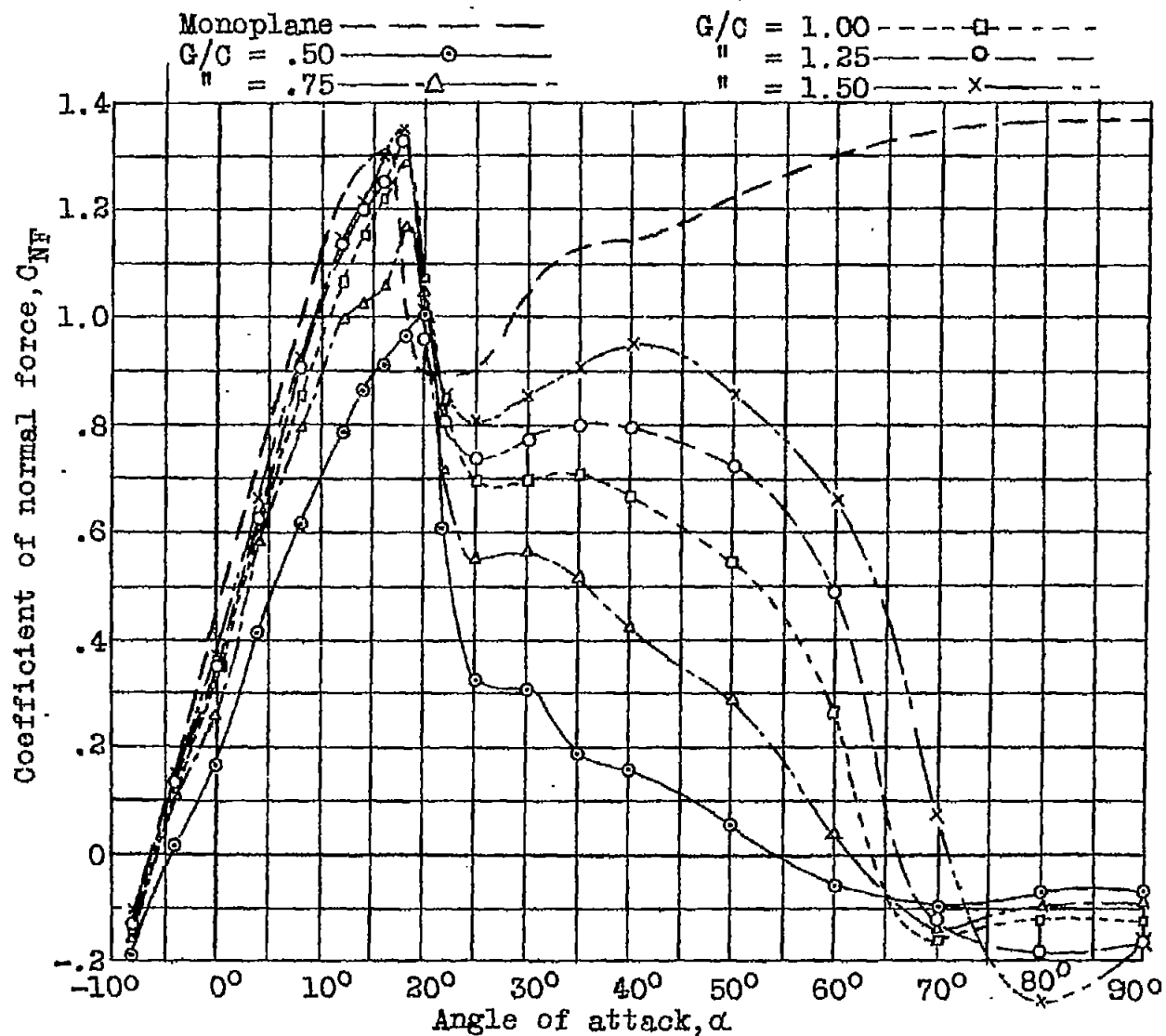


Fig 17 Effect of gap on upper wing normal force coefficient.

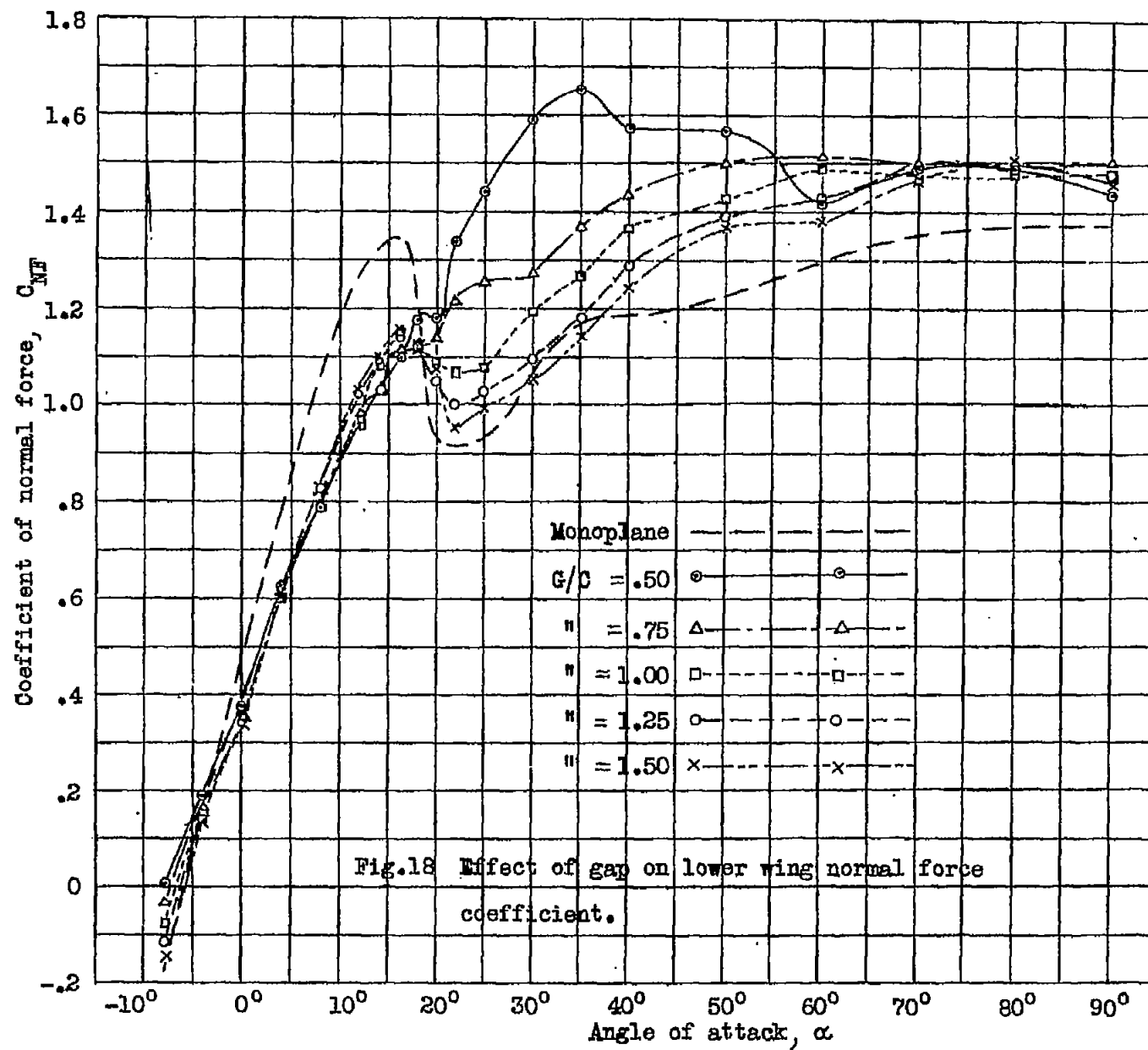


Fig. 18

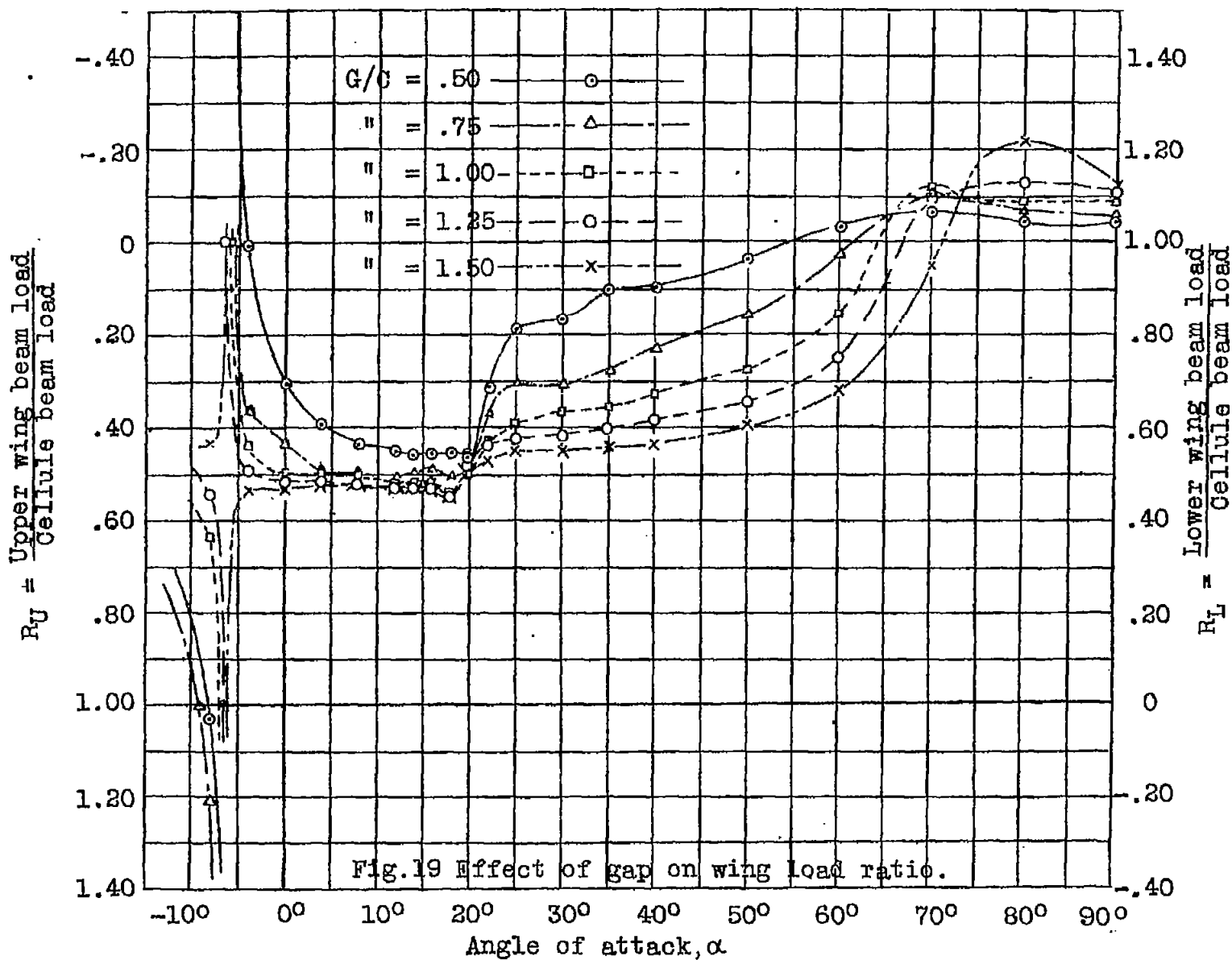
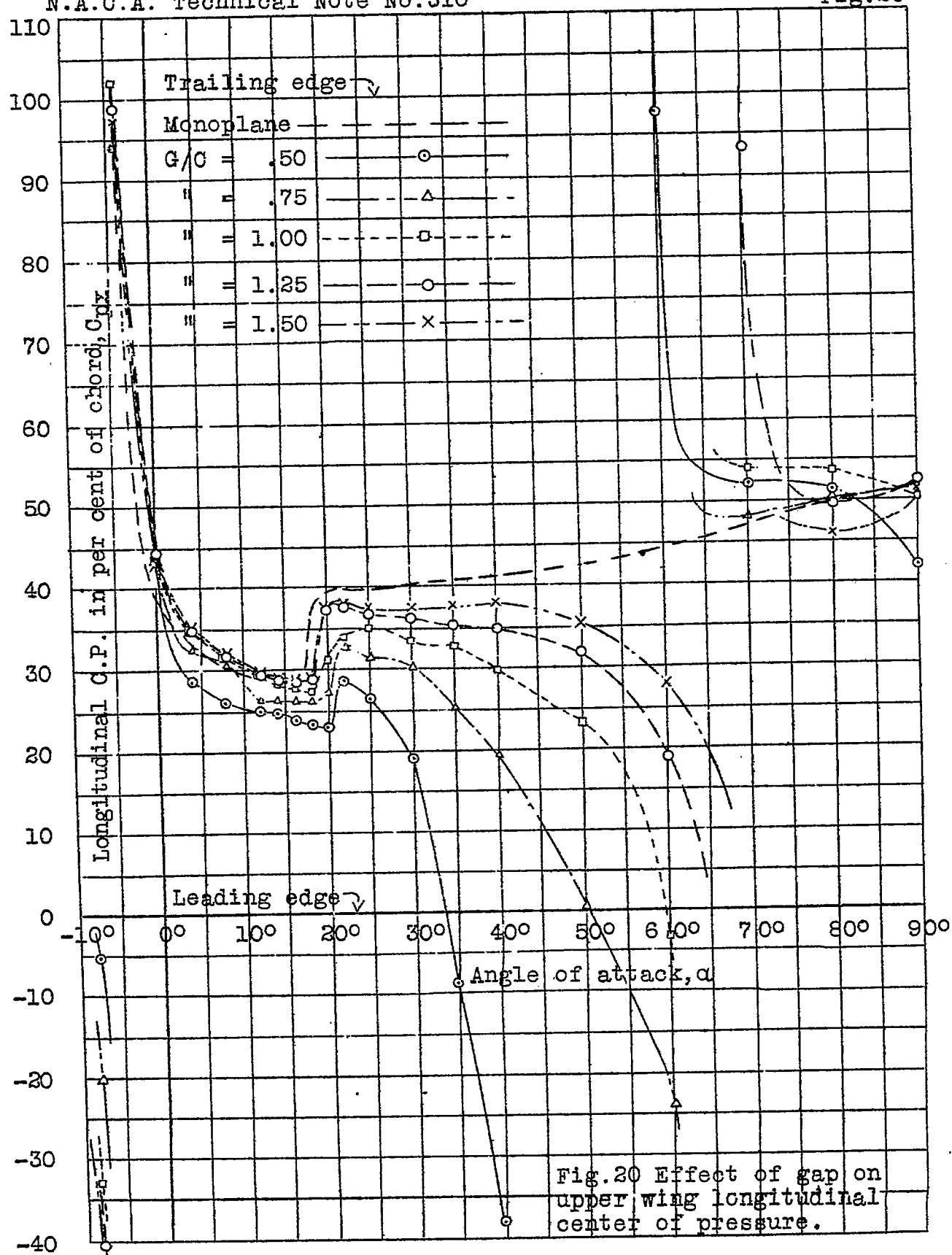
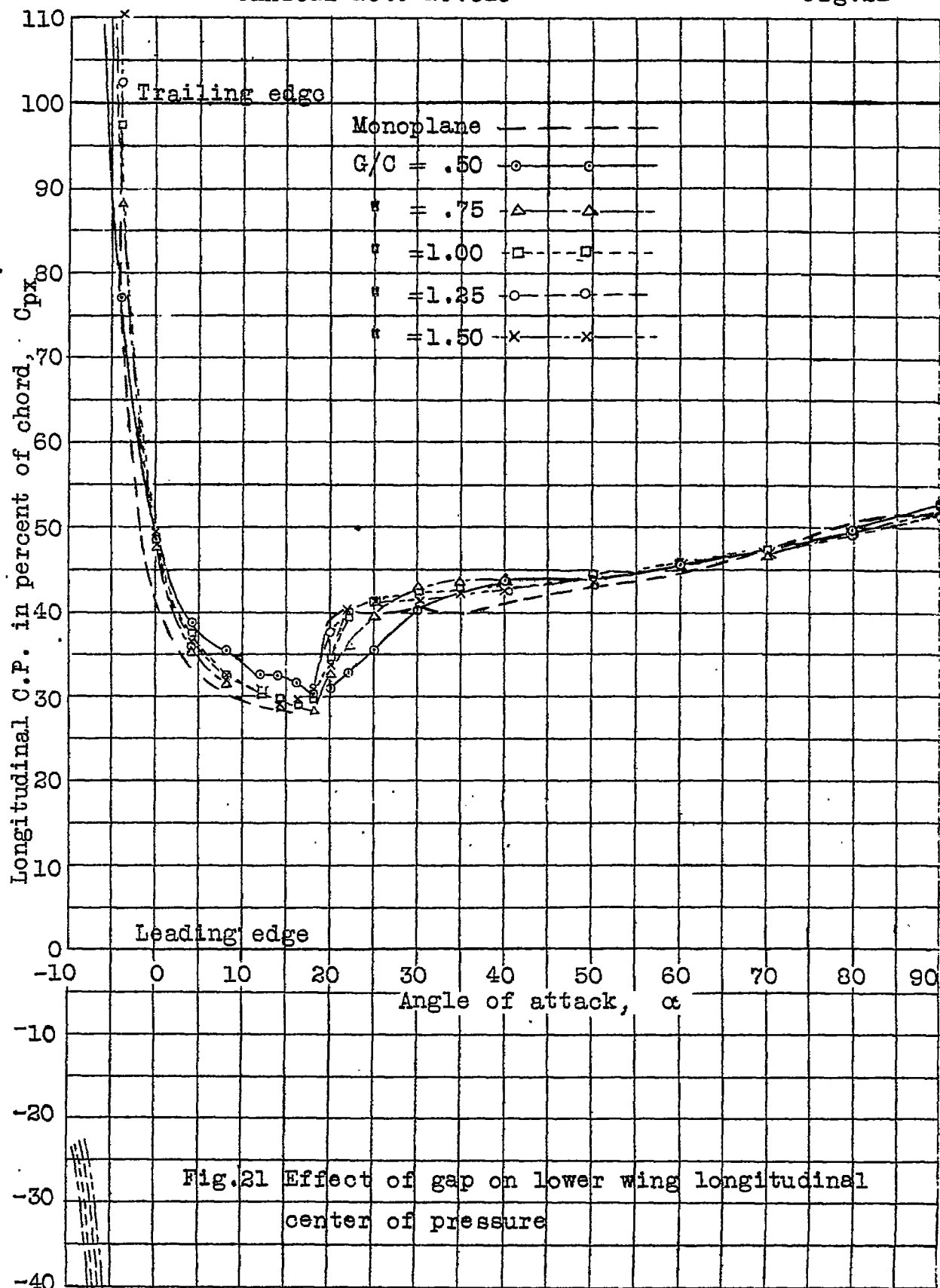


Fig. 19







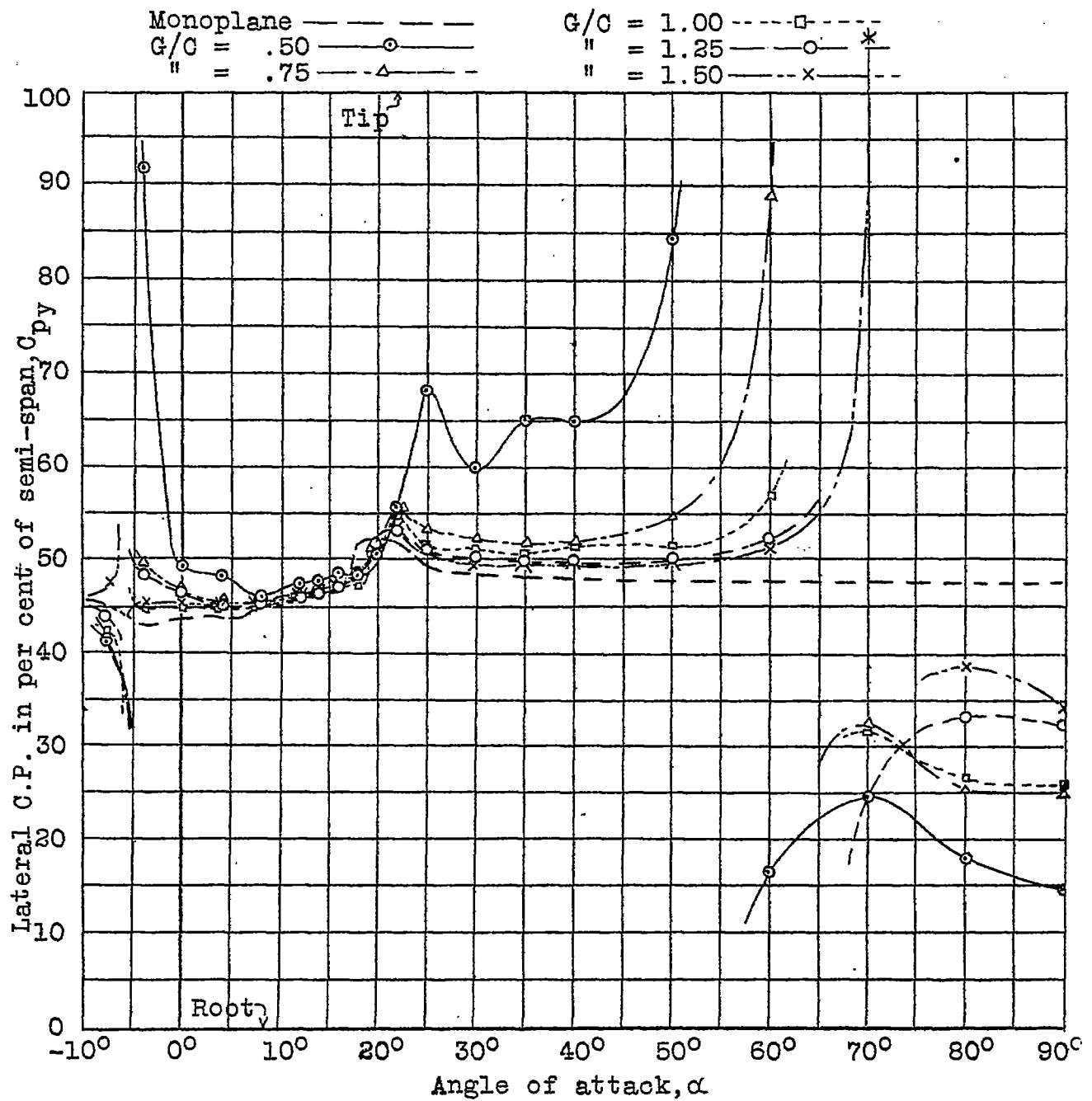


Fig.22 Effect of gap on upper wing lateral center of pressure.

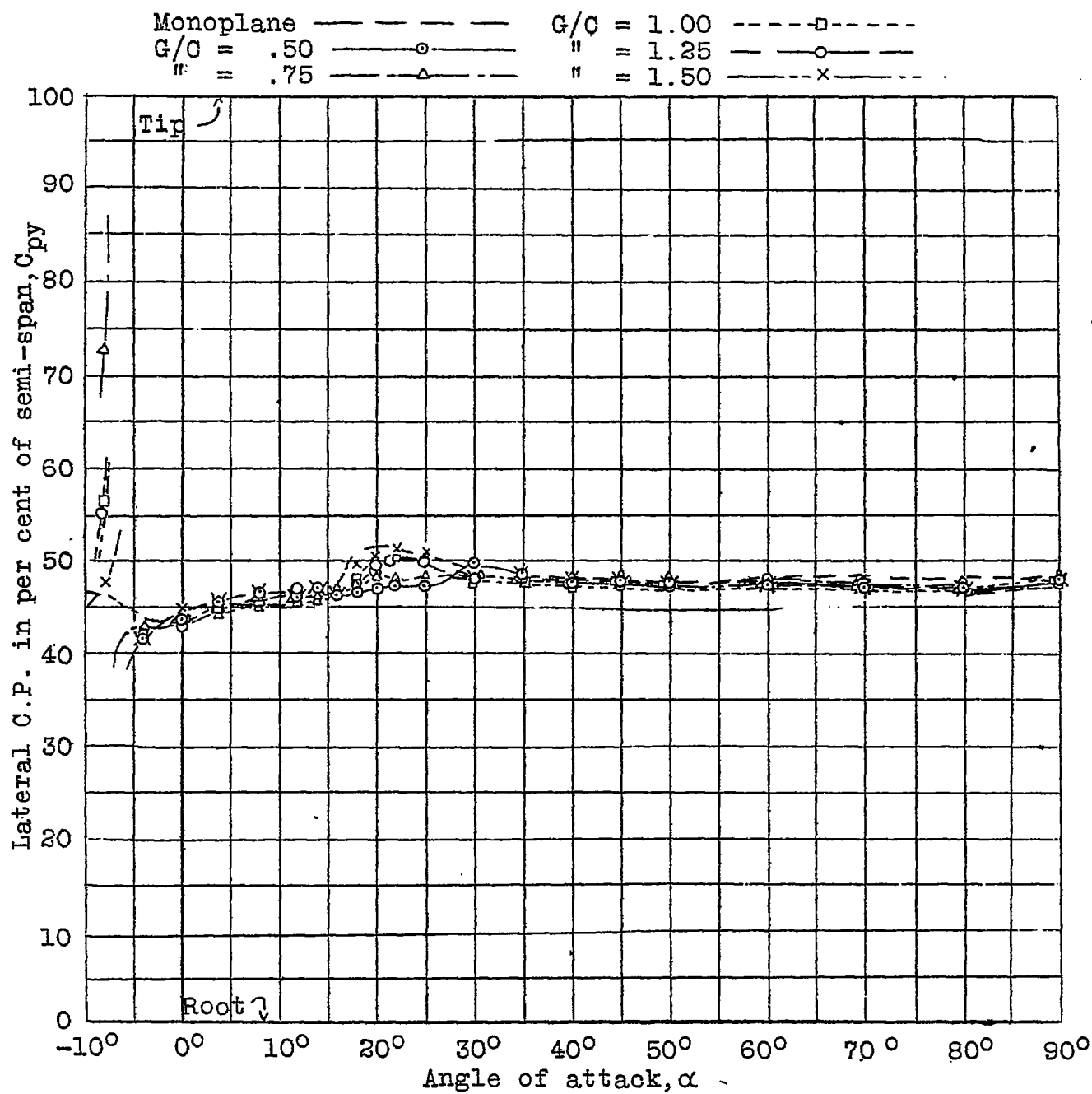


Fig.23 Effect of gap on lower wing lateral center of pressure.